Duplex Dissociation of Telomere DNAs Induced by Molecular Crowding

Daisuke Miyoshi,[†] Shizuka Matsumura,[†] Shu-ichi Nakano,[‡] and Naoki Sugimoto*,[†,‡,§]

Contribution from the Department of Chemistry, Faculty of Science and Engineering, High Technology Research Center, and Frontier Institute for Biomolecular Engineering Research, Konan University, 8-9-1 Okamoto, Higashinada-ku, Kobe 658-8501, Japan

Received June 17, 2003; E-mail: sugimoto@konan-u.ac.jp

Abstract: Because of the importance of telomere DNAs, the structures of these DNAs in vivo are currently of great research interest in the medical, pharmaceutical, chemical, and industrial fields. To understand the structure of biomolecules in vivo, their properties studied in vitro are extrapolated to the in vivo condition, while the condition in a living cell is inherently molecularly crowded and a nonideal solution contains various biomolecules. We investigated the effect of molecular crowding, which is one of the most important cellular environmental conditions, on the structure and stability of the telomere and G-rich and C-rich DNAs using circular dichroism (CD) spectra, CD melting curves, and isothermal titration calorimetry (ITC). The CD spectra and CD melting curves of G-rich DNA, C-rich DNA, and the 1:1 mixture of G-rich and C-rich DNAs showed that each G-rich DNA, C-rich DNA, and the 1:1 mixture form the antiparallel G-quadruplex, I-motif, and duplex, respectively, in the noncrowding condition as previously considered. On the contrary, the G-rich and C-rich DNAs individually form the parallel G-quadruplex and I-motif, respectively, in the molecular crowding condition, and the 1:1 mixture folds into the parallel G-quadruplex and I-motif but does not form a duplex. The ITC measurements indicated that the thermodynamic stability ($\Delta G°_{20}$) of the duplex formation between the G-rich and C-rich DNAs in the noncrowding condition was -10.2 kcal mol^{-1}, while only a small heat change was observed in the ITC measurements in the molecular crowding condition. These ITC results also demonstrated that the molecular crowding condition prevents any duplex formation between G-rich and C-rich DNAs. These results indicate that a structural polymorphism of the telomere DNAs is induced by molecular crowding in vivo.

Introduction

The structures of the G-rich and C-rich DNAs participate in very important biological processes and the on-set mechanism of diseases.[1] For example, the G-rich and its complementary C-rich DNAs are found in biologically essential regions such as the telomere region,[2] the switch for the *c-myc* gene,[3] the tandem repeat regions such as the human insulin gene,[4] the triplet repeat region that can cause a variety of neurological disorders,[5] and the switch region of immunoglobins.[6] If the G-rich and C-rich DNAs fold into nondouble helical structures in vivo, the nondouble helical structures may have critical functional roles in biological processes and diseases. Furthermore, some G-rich DNAs have been discovered as functional molecules such as aptamers and (deoxy)ribozymes.[7] Because of their importance, the structures of these DNAs in vivo are

currently of great scientific interest in the medical, pharmaceutical, chemical, and industrial fields.

Most telomere DNAs are double-stranded between the G-rich and C-rich strands and built up with G−C and A−T Watson−Crick base pairs, except for the 3′ terminal region of the G-rich strand. However, it was revealed that each G-rich or C-rich strand is prone to form a four-stranded helix in vitro; that is, the G-rich strand can fold into a G-quadruplex with coplanar Hoogsteen base pairs,[6,8] while the C-rich strand can form an I-motif containing the hemiprotonated C$^+$·C base pairs.[9] In addition, many researchers have reported that cellular environmental conditions such as pH, cations, and temperature can generate the structural polymorphism of these DNAs.[10] However, the condition in a living cell is inherently molecularly crowded with various biomolecules; the total concentration of the biomolecules inside *Escherichia coli* is in the range of 300−400 g/L.[11] This is distinct from typical biomolecular concentra-

[†] Department of Chemistry.
[‡] High Technology Research Center.
[§] Frontier Institute for Biomolecular Engineering Research.
(1) (a) Neidle, S.; Read, M. A. *Biopolymers* **2001**, *56*, 195−208. (b) Richard H.; Shafer, R. H.; Smirnov, I. *Biopolymers* **2001**, *56*, 209−227.
(2) Blackburn, E. H. *Cell* **1994**, *77*, 621−623.
(3) Evans, T.; Schon, E.; Gora-Maslak, G.; Patterson, J.; Efstratiadis, A. *Nucleic Acids Res.* **1984**, *12*, 8043−8058.
(4) Bell, G. I.; Selby, M. J.; Rutter, W. J. *Nature* **1982**, *295*, 31−35.
(5) Wells, R. D.; Waren, S. T.; Sarmiento, M. *Genetic Instabilities and Hereditary Neurological Diseases*; Academic Press: San Diego, CA, 1998.
(6) Sen, D.; Gilbert, W. *Nature* **1988**, *334*, 364−366.

(7) (a) Macaya, R. F.; Schultze, P.; Smith, F. W.; Roe, J. A.; Feigon, J. *Proc. Natl. Acad. Sci. U.S.A.* **1993**, *90*, 3745−3749. (b) Travascio, P.; Witting, P. K.; Mauk, A. G.; Sen, D. *J. Am. Chem. Soc.* **2001**, *123*, 1337−1348. (c) Forman, S. L.; Fettinger, J. C.; Pieraccini, S.; Gottarelli, G.; Davis, J. T. *J. Am. Chem. Soc.* **2000**, *122*, 4060−4067.
(8) (a) Henderson, E.; Hardin, C. C.; Walk, S. K.; Tinoro, I., Jr.; Blackburn, E. H. *Cell* **1987**, *51*, 899−908. (b) Sundquist, W. I.; Klug, A. *Nature* **1989**, *342*, 825−829.
(9) Kang, C. H.; Berger, I.; Lockshin, C.; Ratliff, R.; Moyzis, R.; Rich, A. *Proc. Natl. Acad. Sci. U.S.A.* **1994**, *91*, 11636−11640.
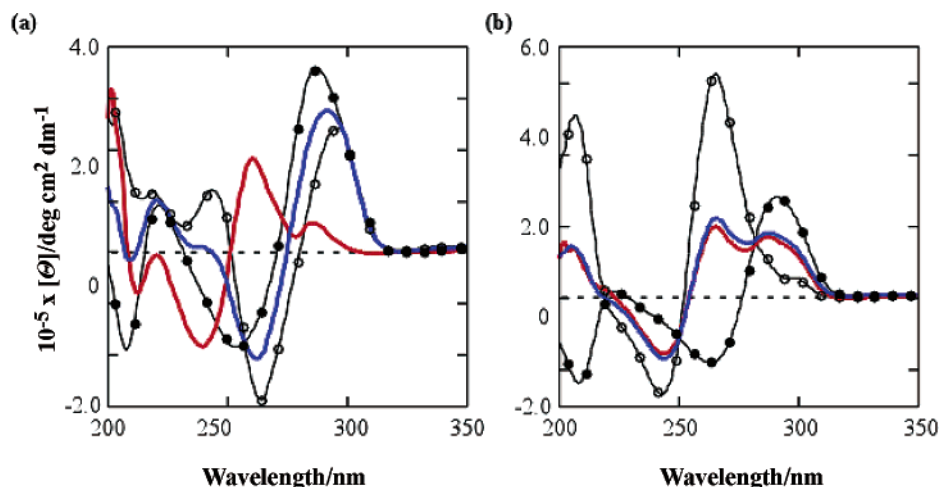
Figure 1. 50 μM GTG (open circle), 50 μM CAC (solid circle), 1:1 mixture of 100 μM GTG/CAC (red), and the sum of CD spectra of GTG and CAC, (GTG + CAC)/2 ((spectra of GTG + spectra of CAC)/2) (blue) in (a) noncrowding and (b) molecular crowding conditions. All measurements were carried out in buffers containing (a) 100 mM NaCl and 50 mM MES (pH 6.1) or (b) 2 M PEG, 100 mM NaCl, and 50 mM MES (pH 6.1) at 5 °C.

tions of less than 1 g/L, which is generally used for experiments in vitro. Furthermore, studies have reported that molecular crowding dramatically stimulates the association between biomolecules and substantially affects the reaction rates.[12] Therefore, the effect of molecular crowding on the structures of the G-rich and C-rich DNAs is critical for revealing these behaviors in vivo and in many biological processes as well as the on-set mechanism of diseases related to these DNAs. Although it has been shown that molecular crowding affects the triple helix DNA,[13] the behaviors of the G-rich and C-rich DNAs, including the telomere DNAs, in a molecular crowding condition are still unknown.

We now report the behavior and thermodynamic properties of the telomere DNA in a molecular crowding condition and find that the molecular crowding generates the structural polymorphism of the DNAs. It has been considered that most telomere DNAs fold into a duplex with Watson−Crick base pairs. However, the results of the circular dichroism (CD) spectra, CD melting curves, and isothermal titration calorimetry (ITC) of the telomere DNAs demonstrated that a duplex, formed between the G-rich and C-rich DNAs in a noncrowding condition, was dissociated by molecular crowding and G-rich and C-rich DNAs folding into quadruplexes. This indicates that the structural polymorphism of the telomere DNAs is induced by molecular crowding in vivo.

Results and Discussion

Structure of G-Rich and C-Rich DNAs in Crowding and Noncrowding Conditions. *Oxytricha nova* telomere DNAs, d(G$_4$T$_4$G$_4$) GTG and d(C$_4$A$_4$C$_4$) CAC, are used as G-rich and C-rich DNAs.[14] To induce the molecular crowding condition, 2 M poly(ethylene glycol) (molecular weight: 300), PEG, was used. Previously, we reported that the interaction between DNA and PEG is thermodynamically unfavorable, and therefore, a specific interaction between DNA and PEG is not formed under a molecular crowding condition.[10c] PEG of 2 M corresponds to 600 g/L that is higher than the total concentration of the biomolecules in a living cell (400 g/L). From these results, it seemed reasonable to use 2 M PEG to induce molecular crowding, although a living cell involves a diversity of molecules. Hall and Minton also reported that the limits of a simplified system and theory mimic the physiological condition in a living cell.[15]

Figure 1a shows the CD spectra of 50 μM GTG, 50 μM CAC, the 1:1 mixture of GTG/CAC (total strand concentration is 100 μM), and the average of the CD spectra of GTG and CAC ((GTG + CAC)/2) in a buffer containing 100 mM NaCl and 50 mM MES (pH 6.1). In this noncrowding condition, the CD spectra of GTG, CAC, and GTG/CAC have a positive peak near 295, 285, and 260 nm, respectively. These spectra show that the structures of GTG, CAC, and GTG/CAC are the G-quadruplex, I-motif, and B-form duplex, respectively.[10b] The spectrum of GTG/CAC is significantly different from that of (GTG + CAC)/2. On the contrary, the CD spectrum of GTG/CAC was identical to that of (GTG + CAC)/2 in a buffer containing 2 M PEG (molecular weight: 300), 100 mM NaCl, and 50 mM MES (pH 6.1) as shown in Figure 1b. This result shows that the 1:1 mixture of GTG/CAC did not form a duplex during the molecular crowding. The CD spectra of GTG and CAC in this molecular crowding condition had positive peaks near 260 and 285 nm, respectively, showing that molecular crowding with PEG induces a parallel G-quadruplex structure of GTG.[10c,d] The CD spectra under these conditions suggest that the duplex dissociation of GTG/CAC is induced by molecular crowding.

(10) (a) Miyoshi, D.; Nakao, A.; Toda, T.; Sugimoto N. *FEBS Lett.* **2001**, *496*, 128−133. (b) Li, W.; Wu, P.; Ohmichi, T.; Sugimoto, N. *FEBS Lett.* **2002**, *526*, 77−81. (c) Miyoshi, D.; Nakao, A.; Sugimoto, N. *Biochemistry* **2002**, *42*, 15017−15024. (d) Miyoshi, D.; Nakao, A.; Sugimoto, N. *Nucleic Acids Res.* **2003**, *31*, 1156−1163. (e) Hardin, C. C.; Watson, T.; Corregan, M.; Bailey, C. *Biochemistry* **1992**, *31*, 833−841. (f) Miura, T.; Thomas, G. *Biochemistry* **1994**, *33*, 7848−7856. (g) Deng, H.; Braunlin, W. *Biopolymers* **1995**, *35*, 677−681. (h) Tuan, A.; Mergny, J.-L. *Nucleic Acids Res.* **2002**, *30*, 4618−4625. (i) Wang, Y.; Patel, D. J. *Structure* **1993**, *1*, 263−282. (j) Parkinson, G. N.; Lee, M. P.; Neidle, S. *Nature* **2002**, *417*, 876−880.

(11) (a) Zimmerman, S. B.; Trach S. O. *J. Mol. Biol.* **1995**, *222*, 599−620. (b) Record, M. T.; Courtenay, E. S.; Cayley D. S.; Guttman, H. J. *Trends Biochem. Sci.* **1998**, *23*, 143−148.

(12) (a) Wenner, J. R.; Bloomfield, V. A. *Biophys. J.* **1999**, *77*, 3234−3241. (b) Minton, A. P. *Curr. Opin. Struct. Biol.* **2000**, *10*, 34−39. (c) Ellis, R. J. *Curr. Opin. Struct. Biol.* **2001**, *11*, 114−119. (d) Minton, A. P. *J. Biol. Chem.* **2001**, *276*, 10577−10580. (e) Shtilerman, M. D.; Ding, T. T.; Lansbury, P. T., Jr. *Biochemistry* **2002**, *41*, 3855−3860.

(13) (a) Spink, C. H.; Chaires, J. B. *J. Am. Chem. Soc.* **1995**, *117*, 12887−12888. (b) Goobes, R.; Minsky, A. *J. Am. Chem. Soc.* **2001**, *123*, 12692−12693.

(14) Pluta, A.; Spear, K. B. *Nucleic Acids Res.* **1982**, *10*, 8145−8154.

(15) Hall, D.; Minton, A. P. *Biochim. Biophys. Acta* **2003**, *1649*, 127−139.
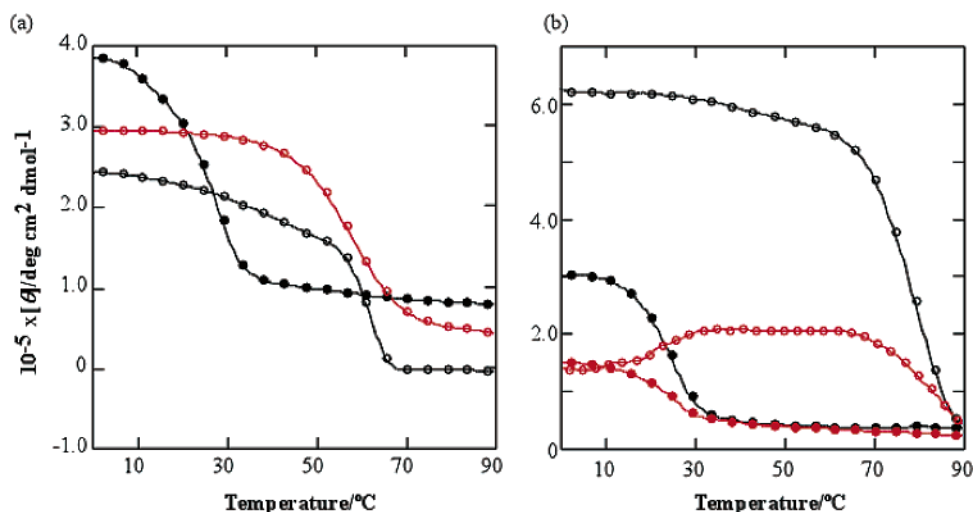
Figure 2. (a) CD melting curves of 50 μM GTG at 295 nm (black open circle), 50 μM CAC at 290 nm (black solid circle), and 100 μM GTG/CAC at 265 nm (red open circle) in the noncrowding condition. (b) CD melting curves of 50 μM GTG at 265 nm (black open circle), 50 μM CAC at 290 nm (black solid circle), 100 μM GTG/CAC at 265 nm (red open circle), and 100 μM GTG/CAC at 290 nm (red solid circle) in the crowding condition. All experiments were carried out in a buffer containing 100 mM NaCl and 50 mM MES (pH 6.1) in the (a) absence and (b) presence of 2 M PEG.

Thermodynamic Stability of Telomere DNAs under the Crowding and Noncrowding Conditions. The thermodynamic stabilities of GTG, CAC, and GTG/CAC under the nonmolecular and molecular crowding conditions were also investigated. Figure 2a shows the CD melting curves of 50 μM GTG at 295 nm, 50 μM CAC at 290 nm, and 100 μM GTG/CAC at 265 nm under the noncrowding condition. These melting curves showed that the melting temperatures, T_m's, of GTG, CAC, and GTG/CAC are 62.5, 26.5, and 58.5 °C, respectively. Each melting curve had a single sigmoidal shape, and the T_m of GTG/CAC was significantly different from that of GTG and CAC. These melting curves and T_m's under the noncrowding condition indicate that the structure of GTG/CAC is the B-form duplex and is not a mixture of the G-quadruplex and I-motif. This melting behavior of GTG/CAC is in contrast to that under the crowding condition as described below. Figure 2b shows the CD melting curves of GTG, CAC, and GTG/CAC under the molecular crowding condition with 2 M PEG. The CD melting curves of the 50 μM GTG at 260 nm and 50 μM CAC at 290 nm showed that the T_m's of GTG and CAC were 81.5 and 25.5 °C, respectively. The CD melting curves of the 100 μM GTG/CAC at 260 and 290 nm showed that the T_m's were 82.5 and 26.0 °C, respectively. The T_m's of GTG at 260 nm and of GTG/CAC at 260 nm were almost the same. Similarly, the T_m's of CAC at 290 nm and of GTG/CAC at 290 nm were almost the same. From a comparison of the thermodynamic stabilities in the noncrowding condition, these thermodynamic stabilities in the molecular crowding condition indicate that GTG and CAC are almost independently unfolded during the thermal denaturation in the case of the GTG/CAC. Therefore, these melting results also show that GTG/CAC folds into the B-form duplex under the noncrowding condition but does not fold into the B-form duplex under the molecular crowding condition. In addition, the melting curve of GTG/CAC at 265 nm under the molecular crowding condition once increased at a lower temerature and decreased at a higher temperature. The mid-temperature of the increase was 24.0 °C, which is slightly lower than the T_m's of CAC at 290 nm and GTG/CAC at 290 nm. Since the CD spectra of the B-form duplex and G-quadruplex have a positive peak around 265 and 260 nm, respectively, as
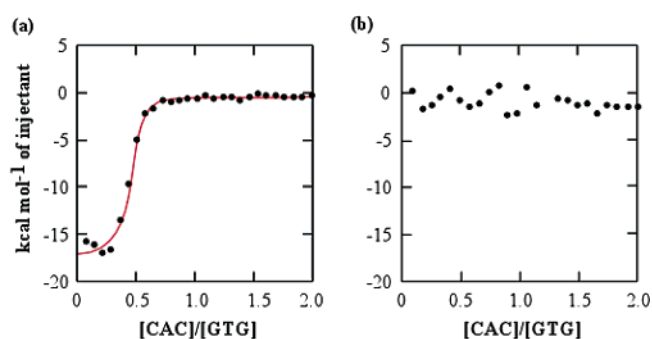

Figure 3. The integrated heats from the ITC data (black circle) and the best-fit curve (solid line) to a 1:1 binding model for the binding between and GTG and CAC in buffers containing 100 M NaCl and 50 mM MES (pH 6.1) in the (a) absence and (b) presence of 2 M PEG. All the measurements were carried out using 2.5 μM GTG and 60 μM CAC at 20 °C.

shown in Figure 1, it is difficult to distinguish the B-form duplex and parallel G-quadruplex using the CD spectra. Therefore, the increasing of the CD intensity of GTG/CAC at 265 nm indicates that a minor part of CAC forms a duplex with GTG after the dissociation of the I-motif structure of CAC.

Furthermore, heat changes caused by the interaction between GTG and CAC were investigated by the ITC measurements to reveal the duplex dissociation by molecular crowding (Figure 3). The heats generated by successive injections were plotted versus the molar ratio of CAC to GTG. The data were fitted to a one-site model to estimate the thermodynamic parameters and the stoichiometry, N, as previously described[16] and are listed in Table 1. The N value of the CAC binding to GTG under the noncrowding condition is 0.41. This may indicate that not only the duplex formation of GTG and CAC but also the other side reactions, such as the triplex formation, quadruplex formations, or both, occurred through the titration experiments in the noncrowding condition. This coincides with the CD spectra of GTG/CAC, which has a very small positive peak around 285 nm, indicating G-quadruplex formation, I-motif formation, or both in the noncrowding condition (Figure 1a). On the contrary,

(16) Miyoshi, D.; Matsumura, S.; Li, W.; Sugimoto, N. *Nucleosides, Nucleotides, Nucleic Acids* **2003**, *22*, 203−221.

Table 1. Thermodynamic Parameters of the Duplex Formation in the Noncrowding Condition at 20 °C

	N	K_a $(10^7 M^{-1})$	$\Delta G°_{20}$ (kcal mol^{-1})	$\Delta H°$ (kcal mol^{-1})	$\Delta S°$ (eu)^a
noncrowding	0.41	4.31	−10.2	−58.9	−166
	(0.01)^b	(0.56)	(0.1)	(0.1)	(2.3)

^{a} eu indicates cal mol^{-1} K^{-1}. ^{b} The error value is in parentheses.
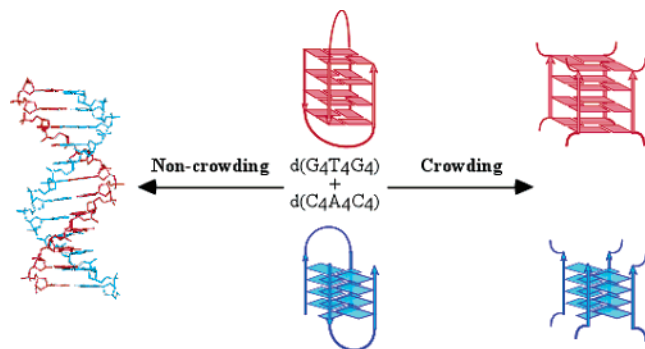
Figure 4. Schematic illustration of the telomere DNA structures in the noncrowding and molecular crowding conditions.

only small heat changes were observed from the ITC measurement in the molecular crowding condition, and thus, the parameters cannot be calculated. This shows that CAC cannot bind to GTG under this condition. These ITC results also demonstrate that the molecular crowding condition prevents the duplex formation of GTG/CAC.

Structural Polymorphisms of Telomere DNAs Induced by Molecular Crowding. It was reported that GTG forms an intermolecular antiparallel G-quadruplex in a noncrowding condition (in the presence of NaCl).[17] It was also reported that d(5mC$_2$T$_3$AC$_2$) and d(C$_4$TGTC$_4$) form a two-stranded I-motif under a noncrowding condition,[18,19] indicating that a C-rich oligonucleotide including two cytosine stretches can form a two-stranded I-motif under the noncrowding condition. Schematic structures of the G-rich and C-rich DNAs in vivo have been proposed on the basis of these results obtained in vitro. However, the effect of molecular crowding reported here on the structures of the telomere DNAs evidently demonstrates that molecular crowding generates and regulates the structural polymorphism of the DNAs. A model of the telomere DNA structures under the noncrowding and crowding conditions are shown in Figure 4. In the noncrowding condition, each GTG, CAC, and GTG/CAC form the antiparallel G-quadruplex, I-motif, and duplex, respectively, as shown in previous reports. On the other hand, GTG and CAC individually form the parallel G-quadruplex and I-motif, respectively, under the molecular crowding condition, and the 1:1 mixture of GTG and CAC folds into the parallel G-quadruplex and I-motif but does not form the duplex. Goobes et al. reported that molecular crowding with PEG (molecular weight: 200−8000) slightly induces a stability to 18-mer duplex.[20] We also found that the stabilities of the DNA duplexes (nontelomere DNAs) shorter than 18-mer do not decrease drastically under a crowding condition (data not shown). These results show that the duplex dissociation of the telomere DNAs

(17) Schulze, P. K.; Smith, F. W.; Feigon, J. *Structure* **1994**, *2*, 221−233.
(18) Nonin, S.; Phan, A. T.; Leroy, J. L. *Structure* **1997**, *5*, 1231−1246.
(19) Catasti, P.; Chen, X.; Deaven, L. L.; Moyzis, R. K.; Bradbury, E. M.; Gupta, G. *J. Mol. Biol.* **1997**, *272*, 369−382.
(20) Goobes, R.; Kahana, N.; Cohen, O.; Minsky, A. *Biochemistry* **2003**, *42*, 2431−2440.

observed in this study is not due to a destabilization of the duplex under the crowding condition. Therefore, the duplex dissociation is induced by the structural changes of GTG and CAC, as will be discussed below.

It was reported that molecular crowding favors the monomer association to form dimers, tetramers, and then polymers because the self-association of biomolecules is progressively facilitated with the increasing extent of crowding and because the magnitude of the crowding effect on self-association increases with the degree of self-association.[15,21] On the basis of this theory, the parallel G-quadruplex structure induced by molecular crowding in this study may be a multi- but not four-stranded parallel structure. Since the CD spectra of the four-stranded and multistranded structures are very similar, the formation of the multistranded parallel G-quadruplex structure is consistent with the CD spectra, as shown in Figure 1. On the other hand, a significant change in the CD spectra of CAC was not observed in the presence and absence of 2 M PEG (Figure 1). However, from the viewpoint of the theory that molecular crowding accelerates multistranded self-association, the crowding condition with 2 M PEG may induce a multistranded parallel I-motif structure of CAC, as shown in Figure 4. Under the noncrowding condition, the I-motif structure of CAC is stabilized by a lower pH because intercalations of C$^+$·C base pairs stabilize the I-motif structure. However, the solubility of CAC decreased, and the aggregation of CAC was observed at lower pHs in the presence of 2 M PEG (data not shown). Although detailed investigations are required to reveal the structure of CAC under the crowding condition, this indicates that the large multistranded parallel I-motif structure of CAC is induced by the lower pHs and molecular crowding.

Significance of the Structural Polymorphism of Telomere DNAs. In this report, we demonstrated that molecular crowding induces the structural polymorphism of the telomere DNAs, in which the antiparallel G-quadruplex of GTG, antiparallel I-motif of CAC, and duplex of GTG/CAC coverted to the parallel G-quadruplex, parallel I-motif, and quadruplexes, respectively. Although a living cell involves a diversity of molecules and the molecular crowding condition used in this study is not the most optimized for a mimic of the cell components, our results indicate an important possibility that the structures of the telomere DNAs investigated in vitro are quite different from those in vivo. This also implies that the correct extrapolation of structures of not only the telomere DNAs but also many biomolecules in vivo from their structures revealed by in vitro experiments is very difficult. From this viewpoint, the effect of molecular crowding, which is one of the most important cellular environmental conditions, on a biomolecular structure is critical and useful to reveal the biomolecular behavior in vivo and to develop an efficient drug and ligand targeting of the telomere DNAs, although there are a few reports that molecular crowding does not drastically affect the protein structure and its stability.[22]

Experimental Section

Materials. All the oligodeoxynucleotides were chemically synthesized on a solid support by the phosphoramidite method as previously described.[23] The synthesized DNA oligonucleotides were removed from the CPG column by treatment with 25% concentrated ammonia at 55

(21) Minton, A. P. *Biopolymers* **1981**, *20*, 2093−2120.
(22) (a) Morar, A. S.; Wang, X.; Pielak, G. J. *Biochemistry* **2001**, *40*, 281−285. (b) Morar, A. S.; Pielak, G. J. *Biochemistry* **2002**, *41*, 547−551.

°C for 8 h. After drying in a vacuum, the DNA oligonucleotides were passed through a Poly-Pak cartridge (Gren Research Co., Ltd.) to remove the dimethoxytrityl groups. After deblocking, the final purities of the DNA oligonucleotides were confirmed to be greater than 98% by HPLC using Wakosil-II 5C18RS cartridges with a linear gradient of 0−50% methanol/water containing 0.1 M TEAA (pH 7.0). These DNA oligonucleotides were desalted with a C-18 Sep-Pack cartridge before use.

The single-strand concentrations of the DNA oligonucleotides were determined by measuring the absorbance at 260 nm at high temperature using a Hitachi U-3210 spectrophotometer connected to an Hitachi SPR-10 thermoprogrammer. The single-strand extinction coefficients were calculated from the mononucleotide and dinucleotide data using the nearest-neighbor approximation.[23]

CD Measurements. A recent conformational analysis of the G-quadruplex structures revealed that the CD spectra of an antiparallel G-quadruplex structure had a positive peak near 295 and a negative peak near 265 nm, while a parallel G-quadruplex structure had positive and negative peaks near 260 and 240 nm, respectively.[24] With this information, the structural type of a G-quadruplex can be determined from the CD measurement. CD experiments utilizing a JASCO J-820 spectropolarimeter were measured for the 50 μM total strand concentration of d($G_4T_4G_4$), 50 μM d($C_4A_4C_4$), and a 100 μM 1:1 mixture of d($G_4T_4G_4$) and d($C_4A_4C_4$) in a 0.1-cm path-length cuvette with buffers containing 50 mM MES (pH 6.1) and 100 mM NaCl in the absence and presence of 2 M PEG at 5 °C. The CD spectra were obtained by taking the average of at least three scans made from 200 to 350 nm. The temperature of the cell holder was regulated by a JASCO PTC-348 temperature controller, and the cuvette-holding chamber was flushed with a constant stream of dry N_2 gas to avoid water condensation on the cuvette exterior. Before the measurement, the sample was heated to 90 °C, gently cooled at the rate of 3 °C min^{-1}, and incubated at 5 °C for several hours.

Melting curves of the antiparallel and parallel G-quadruplexes were measured with the CD intensity at 295 and 260 nm, respectively, because the antiparallel and parallel G-quadruplexes have a significant positive peak at 295 and 260 nm, respectively.[24] Melting curves of the I-motif structure were measured with the CD intensity at 290 nm because the I-motif structure has a positive peak at 290 nm. Melting curves of the 1:1 mixture of GTG and CAC were measured at 265 nm because the B-form duplex has a positive peak at 265 nm. Melting curves of the mixture were also measured at 290 nm because the CD spectrum of the mixture has positive peaks at not only 265 nm, but also at 290 nm in the crowding condition (Figure 1b). Before the CD spectroscopy, all the samples were thermally treated as described above. The heating rate was 1.0 °C min^{-1}.

ITC Measurements. ITC experiments were performed on the duplex formation using a Microcal VP−ITC isothermal titration calorimeter. The titration of 60 μM d($C_4A_4C_4$) on 2.5 μM d($G_4T_4G_4$) was carried out in buffers containing 100 mM NaCl and 50 mM (pH 6.1) in the absence and presence of 2 M PEG at 20 °C. The syringe was rotated at 300 rpm, the time between injections was 600 s, and the injection volume was 5 μL. The reference cell contained distilled and deionized water. Before the experiment, the samples were heated to 90 °C, gently cooled at the rate of 3 °C min^{-1}, and incubated at 20 °C for several hours. The data were analyzed using Origin 5.0 (Microcal software) with an automatically generated baseline.

(23) (a) Sugimoto, N.; Nakano, M.; Nakano, S. *Biochemistry* **2000**, *39*, 11270−11281. (b) Ohmichi, T.; Nakano, S.; Miyoshi, D.; Sugimoto, N. *J. Am. Chem. Soc*. **2002**, *124*, 10367−10372.
(24) (a) Balagurumooty, P.; Brahmachari, S. K.; Mohanty, D.; Bansal, M.; Sasisekharan, V. *Nucleic Acids Res.* **1992**, *20*, 4061−4067. (b) Wyatt, J. R.; Davis, P. D.; Freier, S. M. *Biochemistry* **1996**, *35*, 8002−8008.